

DOI:10.1002/ejic.201402278

A Neutral 1D Coordination Polymer Constructed from the Ni^{II} Complex of the *N*-Phosphorylated Thiourea PhNHC(S)NHP(O)(OPh)₂ and Pyrazine: A Single-Source Precursor for Nickel Nanoparticles



Maria G. Babashkina,^[a] Damir A. Safin,^[a] Koen Robeyns,^[a] and Yann Garcia*^[a]

Keywords: Coordination polymers / Organic–inorganic hybrid composites / Nanoparticles / Nickel / N ligands

The *N*-phosphorylated thiourea PhNHC(S)NHP(O)(OPh)₂ (HL) was synthesized by the reaction of PhNH₂ and (PhO)₂-P(O)NCS. Reaction of the KL salt, generated in situ, with NiCl₂ leads to pale violet [NiL₂] with a 1,3-*N,S*- coordination mode of the ligands. Interaction of [NiL₂] with pyrazine (pz) yields the 1:1 coordination polymer [NiL₂pz]_n. An unexpected change in the coordination mode of the phosphorus-con-

taining ligands **L** from 1,3-*N,S*- to 1,5-*O,S*- was found in [NiL₂pz]_n upon coordination of additional donor ligands. [NiL₂pz]_n dissolved in tri-*n*-octylphosphine (TOP) was decomposed in hot hexadecylamine to give capped face-centered cubic Ni nanoparticles with an average particle size of 17(2) nm.

Introduction

There is currently an intense activity in the synthesis and design of coordination polymers (CPs) and metal–organic frameworks (MOFs).^[1] Such compounds belong to an intriguing class of hybrid materials, comprising inorganic nodes and organic ligands linked by coordination interactions,^[2] exhibiting valuable properties, which were used in a wide range of fields,^[3] including MRI contrast agents,^[4] adsorption heat pump processes,^[5] and so on. In terms of crystal engineering of CPs, didentate π -electron-containing ligands are of ever increasing interest. Among them, pyrazine (pz) and its close analogue 4,4'-bipyridine are the most commonly used tectons for the formation of CPs.^[6] Furthermore, pz-containing complexes are used in electron transfer and magnetic exchange interaction studies,^[7] thanks to the capacity of pz to yield complexes with short metal–metal distances.

A great number of Ni^{II} complexes with the imidodiphosphinates R₂P(X)NHP(Y)R'₂ (IDP) (X, Y = O, S, Se, Te),^[8] acylthioamides RC(S)NHC(X)R' (AA), and aroylthioureas R₂NC(S)NHC(X)R' (ATU) (X = O, S)^[9] have been described. The chelate backbones of the IDP, AA, and ATU ligands are coordinated to the Ni^{II} cation through the do-

nor X and Y atoms. This is, obviously, explained by the efficient delocalization of the negative charge in the symmetrical conjugated chelate backbone upon deprotonation. Contrariwise, the coordination mode of *N*-(thio)phosphorylated thioamides and thioureas RC(S)NHP(X)(OR')₂ (X = O, S), which are asymmetrical analogues of IDP, AA, and ATU, to Ni^{II} still remains less studied. This is rather surprising, as the negative charge is delocalized asymmetrically in these deprotonated ligands, and hence they might show ambidental coordination properties through the donor atoms of the thiocarbonyl and (thio)phosphoryl groups and the nitrogen atom of the phosphorylamide group. Furthermore, the nature of the R and R' substituents might influence considerably the coordination mode by both electronic and steric factors. Additional donor functions in these substituents might also affect the complexation properties crucially.

In this context, we have studied the coordination properties of *N*-(thio)phosphorylated thioureas RR'NC(S)NHP(X)(OR')₂ (X = O, S; R, R' = H, alkyl, aryl; R'' = OiPr, OPh) (NTTU) towards Ni^{II} and demonstrated that their square-planar complexes exhibit either a 1,3-*N,S*- or 1,5-*O,S*- and 1,5-*S,S'*- coordination mode.^[10] Furthermore, we also examined the interaction of the formed mononuclear Ni^{II} complexes of NTTU with additional chelate donor ligands, such as 2,2'-bipyridine and 1,10-phenanthroline, and showed that the coordination mode is preserved for the phosphorus-containing ligands.^[10e] Thus, inspired by our recent findings, we have prepared a new CP, using a mononuclear homoleptic Ni^{II} complex of the *N*-phosphorylated thiourea PhNHC(S)NHP(O)(OPh)₂ (HL) as an inor-

[a] Institute of Condensed Matter and Nanosciences, Molecules, Solids and Reactivity (IMCN/MOST), Université Catholique de Louvain, Place L. Pasteur 1, 1348 Louvain-la-Neuve, Belgium
E-mail: yann.garcia@uclouvain.be
<http://www.uclouvain.be/262038.html>

Supporting information for this article is available on the WWW under <http://dx.doi.org/10.1002/ejic.201402278>.

ganic node and pz as a bridging organic linker. Furthermore, the resulting CP $[\text{Ni}\{\text{PhNHC}(\text{S})\text{NP}(\text{O})(\text{OPh})_2\}_2\text{pz}]_n$ ($[\text{NiL}_2\text{pz}]_n$) was used as single-source precursor for the preparation of face-centered cubic nickel nanoparticles by using an organic surfactant.

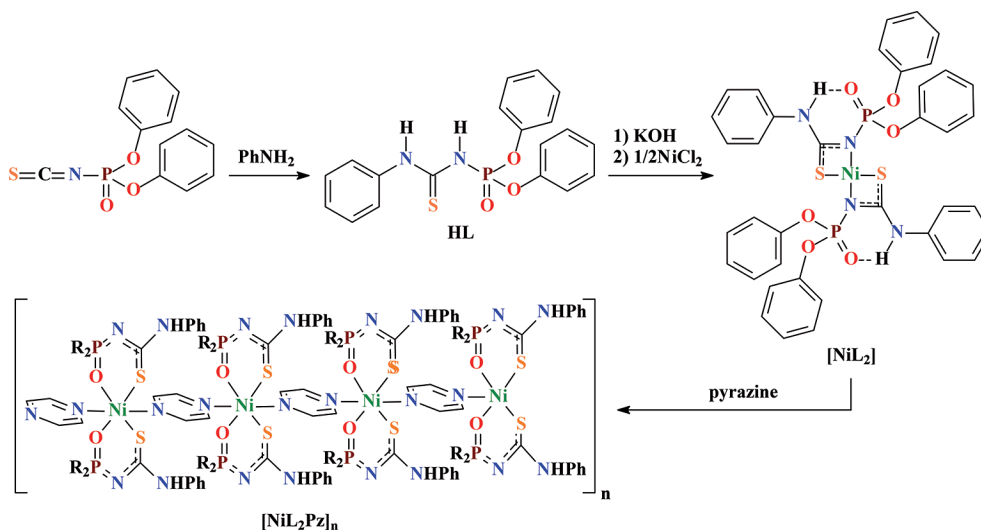
Results and Discussion

The *N*-phosphorylated thiourea HL was synthesized by reacting PhNH_2 with the isothiocyanate $(\text{PhO})_2\text{P}(\text{O})\text{NCS}$ (Scheme 1). Complex $[\text{NiL}_2]$ was prepared by deprotonating the ligand in situ with KOH, followed by reaction with NiCl_2 (Scheme 1). $[\text{NiL}_2\text{pz}]_n$ was synthesized by reacting $[\text{NiL}_2]$ with an equimolar amount of pz in benzene (Scheme 1).

The IR spectrum of HL contains a band at 1241 cm^{-1} for the $\text{P}=\text{O}$ group. The same band in the IR spectrum of $[\text{NiL}_2]$ was observed almost at the same wavenumber (1235 cm^{-1}) as that for the parent ligand HL, while it is significantly shifted to lower frequencies (1135 cm^{-1}) in the spectrum of $[\text{NiL}_2\text{pz}]_n$. The latter observations testify to a 1,3-*N,S*- and 1,5-*O,S*- coordination mode of the deprotonated ligand L in the structures of $[\text{NiL}_2]$ and $[\text{NiL}_2\text{pz}]_n$, respectively.^[10] In the spectrum of HL, there is a weak band at 1548 cm^{-1} , corresponding to the $\text{S}=\text{C}-\text{N}$ fragment, while the spectra of its complexes contain an intense broad band at 1560 and 1673 cm^{-1} , respectively, due to the conjugated $\text{S}=\text{C}=\text{N}$ fragment. The spectrum of HL contains bands at 3155 and 3294 cm^{-1} , corresponding to the PhNH and NHP groups. The IR spectra of $[\text{NiL}_2]$ and $[\text{NiL}_2\text{pz}]_n$ contain the characteristic band for the PhNH group at 3257 and 3184 cm^{-1} , while no bands for the NHP groups are found. This testifies to a deprotonated form of the phosphorus ligands in the structures of the complexes. In addition, in the IR spectra of HL, $[\text{NiL}_2]$, and $[\text{NiL}_2\text{pz}]_n$, there is a broad, intense band arising from the POC group at 956 – 978 cm^{-1} .^[11]

The $^{31}\text{P}\{^1\text{H}\}$ NMR signal of HL in $[\text{D}_6]\text{DMSO}$ appears as a singlet at $\delta = -10.2$ ppm. The ^1H NMR spectrum of HL in the same solvent contains a multiplet signal for the Ph protons at $\delta = 7.02$ – 7.66 ppm and two singlets at 9.98 and 10.25 ppm, corresponding to the NHP and PhNH groups, respectively. The $^{31}\text{P}\{^1\text{H}\}$ NMR spectrum of $[\text{NiL}_2]$ in CDCl_3 contains a singlet signal at $\delta = -7.8$ ppm, while in $[\text{D}_6]\text{DMSO}$ this signal is shifted to low field and observed at $\delta = -5.4$ ppm. These findings are very similar to those observed for the close analogue $[\text{Ni}\{i\text{PrNHC}(\text{S})\text{NP}(\text{O})(\text{OPh})_2\}_2]$ ^[10a] and testifies to the formation of $[\text{Ni}(\text{L}-1,3-\text{N},\text{S})_2]$ and $[\text{Ni}(\text{DMSO}-\text{O})_2(\text{L}-1,3-\text{N},\text{S})_2]$ upon dissolving $[\text{NiL}_2]$ in CDCl_3 and $[\text{D}_6]\text{DMSO}$, respectively. It should be noted that anionic ligands L in these structures are coordinated in a *trans*-arrangement. The ^1H NMR spectrum of $[\text{NiL}_2]$ in CDCl_3 is similar to that of the parent ligand HL. The phenyl and PhNH protons are found at 7.32–8.04 and 9.15 ppm, respectively. The ^1H NMR spectrum of $[\text{NiL}_2]$ in $[\text{D}_6]\text{DMSO}$ also contains a single set of signals. Although the signals for the Ph protons are in the characteristic range at $\delta = 6.92$ – 7.71 ppm, the singlet for the PhNH protons is observed at $\delta = 5.07$ ppm, which is an unusual chemical shift for such a type of protons.^[10] This might be explained by the paramagnetic contribution of the $[\text{Ni}(\text{DMSO}-\text{O})_2(\text{L}-1,3-\text{N},\text{S})_2]$ structure formed upon dissolving $[\text{NiL}_2]$ in $[\text{D}_6]\text{DMSO}$. The NMR spectra of $[\text{NiL}_2\text{pz}]_n$ in CDCl_3 and $[\text{D}_6]\text{DMSO}$ are very similar. The $^{31}\text{P}\{^1\text{H}\}$ NMR spectra contain a singlet at an extremely low-field region at about 25 ppm. This might be explained by the change of the coordination mode of the phosphorus-containing ligands and the formation of paramagnetic $\text{NiN}_2\text{O}_2\text{S}_2$ coordination cores in the structure of $[\text{NiL}_2\text{pz}]_n$. The ^1H NMR spectra exhibit signals at 4.18–4.37, 5.27–6.74, and 9.13–10.07, corresponding to the PhNH, Ph, and pz protons, respectively.

UV/Vis absorption spectra of $[\text{NiL}_2]$ in CH_2Cl_2 and DMSO contain two intense absorption bands in the UV region, one lying invariantly at 249–260 nm, and the other



Scheme 1. Preparation of HL, $[\text{NiL}_2]$, and $[\text{NiL}_2\text{pz}]_n$ ($\text{R} = \text{OPh}$).

at 303–321 nm. Notably, these two bands in the spectrum for the sample in CH₂Cl₂ exhibit bathochromic shifts compared to the spectrum for the sample in DMSO. Furthermore, the latter band is about 7.5 times less intense in the spectrum for the sample in DMSO compared to that in the spectrum for the sample in CH₂Cl₂. The UV absorptions of [NiL₂] in both solvents can be assigned to the corresponding intraligand transitions (π - π^* or n - π^* type). In the visible region, two absorption bands were essentially observed in the UV/Vis spectrum for the sample in CH₂Cl₂, one at 508 nm and another rather invariant one at 630 nm. From the rather low intensities ($\epsilon = 218$ and $185 \text{ M}^{-1} \text{ cm}^{-1}$, respectively) the two long-wavelength bands are assigned to ligand field (d-d) transitions. The UV/Vis spectrum of [NiL₂] in DMSO exhibits three bands with maxima at 440, 726, and 1124 nm in the visible range, which are assigned to ${}^3\text{B}_{1g} \rightarrow {}^3\text{E}_g(\text{P})$, ${}^3\text{A}_{2g}(\text{P})$, ${}^3\text{B}_{1g} \rightarrow {}^3\text{E}_g(\text{F})$, ${}^3\text{A}_{2g}(\text{F})$, and ${}^3\text{B}_{1g} \rightarrow {}^3\text{E}_g$, ${}^3\text{B}_{2g}$, respectively, assuming an octahedral environment for the nickel atom in [NiL₂]^[12] due to the formation of [Ni(DMSO-O)₂(L-1,3-*N,S*)₂] species. Furthermore, the band intensities ($\epsilon = 65$, 12, and $15 \text{ M}^{-1} \text{ cm}^{-1}$, respectively) also unambiguously favor the octahedral coordination core rather than the tetrahedral one.^[12] The absorption spectra of [NiL₂pz]_n in the two solvents are very similar and testify to the exclusive formation of an octahedrally configured structure.

Crystals of HL were obtained by recrystallization from a mixture of CH₂Cl₂ and *n*-hexane, while crystals of [NiL₂pz]_n were obtained by slow concentration of its benzene solution. Unfortunately, numerous attempts to obtain crystals of [NiL₂] suitable for X-ray diffraction analysis failed.

The molecular structures of HL and [NiL₂pz]_n are shown in Figure 1 and Figure 2, respectively, while the crystal and structure refinement data are given in the Experimental Section. Selected bond lengths and angles of the complexes are given in Tables S1 and S2 in the Supporting Information. According to X-ray diffraction data, HL and [NiL₂pz]_n, measured at 150(2) K, crystallize in the monoclinic *P*2₁/*c* and triclinic *P* $\bar{1}$ space groups, respectively.

Lengths of the C=S, C-N, P-N and P=O bonds observed for HL are in the typical range for NTTU (X = O) (Table S1 in the Supporting Information).^[10,13] The S=C-N-P=O backbones in the crystal phase have a *cis* conformation (Figure 1). The crystal structure of HL is stabilized by intermolecular bifurcated hydrogen bonds of the PhN-H \cdots O=P and PN-H \cdots O=P types (Figure 1 and Table S3 in the Supporting Information). As a result of these hydrogen bonds, 1D polymeric chains are formed.

Complex [NiL₂pz]_n comprises [NiL₂] building units linked through bridging 1,4-*N,N'*-coordinated pz molecules with the formation of an infinite 1D neutral CP (Figure 2). Surprisingly, the ligands L now exhibit a 1,5-*O,S*- coordination mode. Furthermore, the anionic ligands are coordinated in a *cis* arrangement. To the best of our knowledge, [NiL₂pz]_n is the first example of Ni^{II} complexes with NTTU (X = O), exhibiting a *cis*-1,5-*O,S*- coordination mode. Recently, a *cis*-1,5-*S,S'*- coordination mode was found in the structure of [Ni{AdNHC(S)NP(S)(O*i*Pr)₂}₂].^[10c] Neighboring [NiL₂] building units are linked by pz molecules in a *trans* arrangement, which might be influenced by the bulky PhO groups at the phosphorus atoms (Figure 1). The coordination polyhedron around the metal center is best described as a distorted octahedron. The Ni \cdots Ni separations between the neighboring metal centers are about 7.06 Å. The Ni-N bond lengths in the structure of [NiL₂pz]_n are very similar and about 2.18 Å, while the Ni-O and Ni-S bonds, arising from two different ligands L coordinated to the same metal center, show the opposite trend (Table S2 in the Supporting Information). Thus, the Ni1-O6 bond is about 0.17 Å longer than the Ni1-O36 bond, while the Ni1-S2 distance, corresponding to the same ligand L as the former Ni-O bond, is about 0.11 Å shorter than that of Ni1-S32. This trend is also reflected in the S-C and P-O bonds in the structures of L. However, although the S2-C3 bond is about 0.19 Å longer than the S32-C33 bond, which, in turn, has the same value as that in the structure of the parent ligand HL (Table S1 in the Supporting Information), the P-O bonds are very similar and are about 1.52 Å (Table S2 in the Supporting Information). The

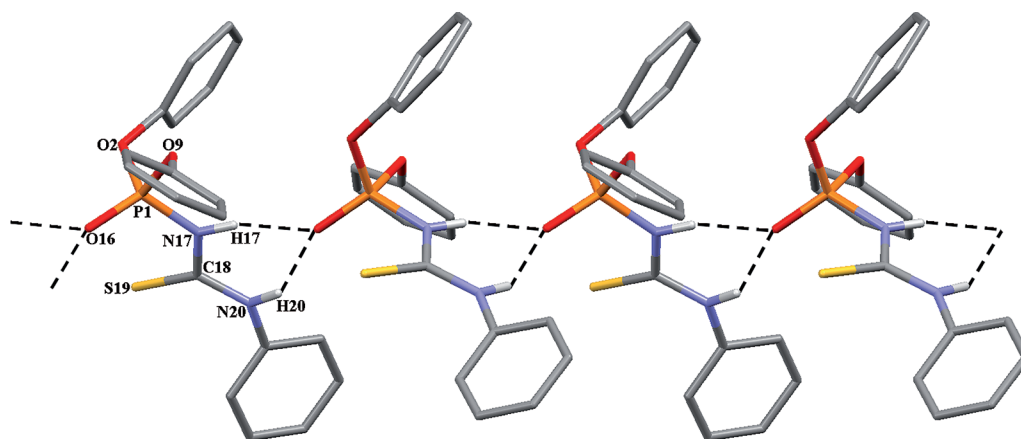


Figure 1. Stick plot of HL along the *ob* axis. Hydrogen atoms, not involved in hydrogen bonding, were omitted for clarity.

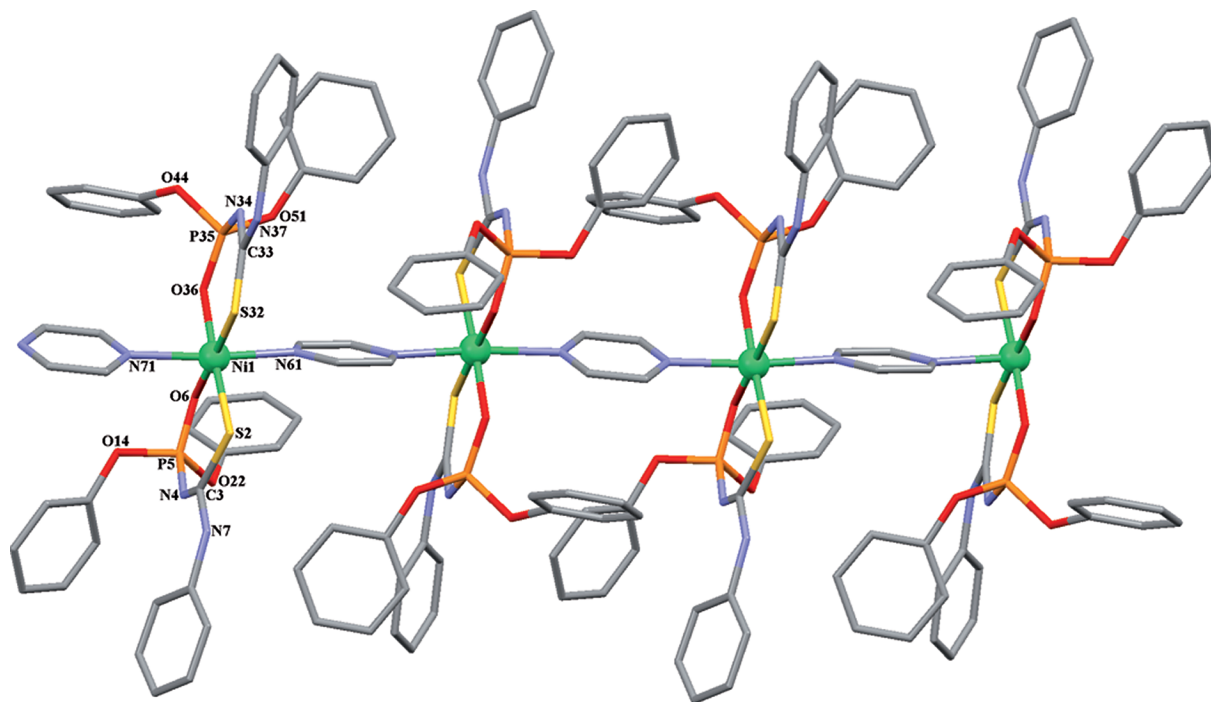


Figure 2. Stick plot of **1** along the $0c$ axis. Hydrogen atoms were omitted for clarity.

latter bond lengths are almost the same as those in HL. The P35–N34 and N34–C33 bonds are similar to those observed for HL, while they are significantly elongated relative to the P5–N4 and N4–C3 distances (Table S2 in the Supporting Information). On the contrary, the N7–C3 bond is very similar, while the N37–C33 bond is about 0.14 Å longer in comparison to the same bond in the structure of HL. The six-membered metallacycles Ni–S–C–N–P–O are almost flattened with the Ni1, O6, and S2 atoms in one cycle, and Ni1 and O36 atoms in the other one, deviate by about 0.15 Å from the least-squares planes. The N–Ni–N angle, 167.7(11)°, deviates slightly from the linear, while the external interligand angles S–Ni–O are almost linear with values of about 176 and 180° (Table S2 in the Supporting Information). The remaining O–Ni–N, S–Ni–N, S–Ni–O, O–Ni–O, and S–Ni–S angles around the metal center are close to 90°. The torsion angle between the planes formed by pz rings is about 13.9°, while the planes formed by the six-membered metallacycles are almost orthogonal to the pz planes (ca. 79.3–84.5°). The structure of $[\text{NiL}_2\text{pz}]_n$ is additionally stabilized by close interchain $\pi\cdots\pi$ stacking interactions between the OPh phenylene rings corresponding to neighboring CPs (Figure 3, Table S4 in the Supporting Information).

We have also been interested in the possible formation of Ni-containing nanoparticles from both $[\text{NiL}_2]$ and $[\text{NiL}_2\text{pz}]_n$. Face-centered cubic (fcc) Ni nanoparticles were obtained when $[\text{NiL}_2\text{pz}]_n$ was used as single-source precursor by following our recently reported procedure.^[10m] However, using $[\text{NiL}_2]$ as a precursor for preparing nanoparticles resulted in a mixture of different products and requires more detailed analysis, which will be reported in due course.

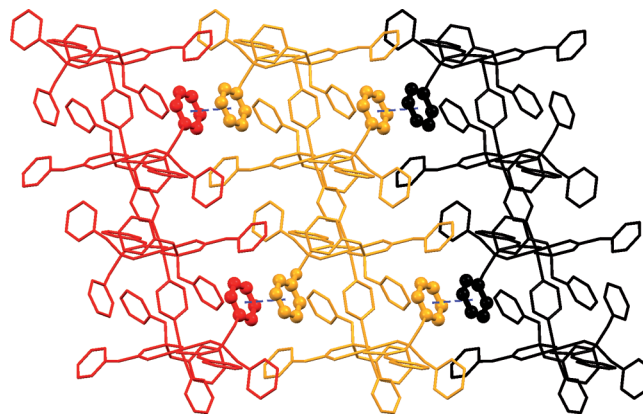


Figure 3. Ball and stick plot of $\pi\cdots\pi$ stacking interactions between 1D polymeric chains of **1** along the $0b$ axis. Hydrogen atoms were omitted for clarity.

The reduction of $[\text{NiL}_2\text{pz}]_n$, dissolved in tri-*n*-octylphosphine (TOP), at 190 °C in hexadecylamine (HDA) resulted in a fast reaction of the nickel complex and the growth of nickel nanoparticles. The transmission electron microscopy (TEM) image (Figure 4A) shows that the TOP-capped nickel nanoparticles afford an average particle size of 17(2) nm. We conclude that a compact layer of TOP is formed between the nickel nanoparticles to prevent them from aggregation, confirming TOP to be an effective surfactant for producing well-dispersed metal nanoparticles. The lattice fringes with an interplanar distance of 3.53 Å are visible in the HRTEM image (Figure 4B). The X-ray diffraction (XRD) pattern indicates three peaks (111), (200), and (220) above $2\theta = 30^\circ$, which are characteristic of fcc

nickel with a lattice constant of $a = 3.538 \text{ \AA}$ (Figure 4). This value is consistent with the corresponding bulk value.^[14] To investigate the composition, X-ray photoelectron spectrometry (XPS) analyses were performed for the Ni nanoparticles (Figure 4). The Ni $2p_{3/2}$ and Ni $2p_{1/2}$ are centered at 853.2 and 869.6 eV, respectively; these peaks coincide with those of metallic Ni.^[15] Therefore, on the basis of XRD and XPS results, it can be concluded that the synthesized Ni nanoparticles have the component of pure metallic Ni phase.

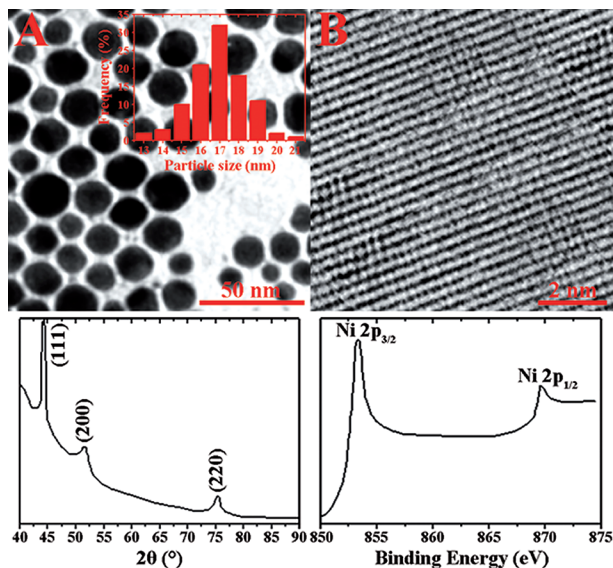


Figure 4. TEM (A), HRTEM (B) images, XRD pattern (bottom left), and XPS spectrum (bottom right) of TOP-capped Ni nanoparticles synthesized from 0.2 mmol $[\text{NiL}_2\text{pz}]_n$.

Conclusions

In summary, we have synthesized a homoleptic Ni^{II} complex with *N*-thiophosphorylated thiourea $\text{PhNHC}(\text{S})\text{NHP}(\text{O})(\text{OPh})_2$, $[\text{NiL}_2]$. In both the solid state and in CDCl_3 and CH_2Cl_2 solutions, the complex exhibits a square-planar 1,3-*N,S*- coordination mode of the ligands, while an octahedral coordination environment, formed by two 1,3-*N,S*-coordinated phosphorus ligands and two molecules of the solvent, was established in DMSO.

$[\text{NiL}_2]$ was involved in the reaction with pyrazine to form of a 1D coordination polymer $[\text{NiL}_2\text{pz}]_n$. An unexpected change in the coordination mode of L from 1,3-*N,S*- to 1,5-*O,S*- was observed in the latter complex upon coordination of additional donor ligands.

We have also demonstrated that the coordination polymer $[\text{NiL}_2\text{pz}]_n$ dissolved in tri-*n*-octylphosphine decomposes in hot hexadecylamine to give capped face-centered cubic Ni nanoparticles with an average particle size of 17(2) nm. These nanoparticles retain their shape over long periods and also their monodispersity, a finding which could be of interest in catalysis.^[16]

Experimental Section

Physical Measurements: Infrared spectra (KBr) were recorded with a FTIR-8400S SHIMADZU spectrophotometer in the range 400–3600 cm^{-1} . NMR spectra were obtained with a Bruker Avance 300 MHz spectrometer at 25 °C. ^1H and $^{31}\text{P}\{^1\text{H}\}$ NMR spectra were recorded at 299.948 and 121.420 MHz, respectively. Chemical shifts are reported with reference to SiMe_4 (^1H) and 85% H_3PO_4 ($^{31}\text{P}\{^1\text{H}\}$). Electronic absorption spectra were recorded with a Perkin–Elmer Lambda 35 spectrophotometer. X-ray powder diffraction (XRPD) studies were performed with a Bruker AXS D8 diffractometer by using $\text{Cu-K}\alpha$ radiation. Transmission electron microscopy (TEM) was performed with a Philips CM 20 FEG electron microscope. X-ray photoelectron spectrometry (XPS) analysis was performed with a Shimadzu ESCA-3400 instrument. Elemental analyses were performed with a Thermoquest Flash EA 1112 Analyzer from CE Instruments.

HL: A solution of aniline (0.465 g, 5 mmol) in anhydrous CH_2Cl_2 (15 mL) was treated under vigorous stirring with a solution of $(\text{PhO})_2\text{P}(\text{O})\text{NCS}$ (1.746 g, 6 mmol) in the same solvent. The mixture was stirred for 1 h. The solvent was removed in a vacuum, and the product was purified by recrystallization from a 1:5 (v/v) mixture of CH_2Cl_2 and *n*-hexane. Yield: 1.653 g (86%). IR: $\tilde{\nu} = 978$ (POC), 1241 (P=O), 1548 (S=C–N), 3155, 3294 (NH) cm^{-1} . ^1H NMR ($[\text{D}_6]\text{DMSO}$): $\delta = 7.02$ – 7.66 (m, 15 H, Ph), 9.98 (br. s, 1 H, NHP), 10.25 (s, 1 H, PhNH) ppm. $^{31}\text{P}\{^1\text{H}\}$ NMR ($[\text{D}_6]\text{DMSO}$): $\delta = -10.2$ ppm. $\text{C}_{19}\text{H}_{17}\text{N}_2\text{O}_3\text{PS}$ (384.39): calcd. C 59.37, H 4.46, N 7.29; found C 59.42, H 4.49, N 7.17.

$[\text{NiL}_2]$: A suspension of HL (3 mmol, 1.153 g) in MeOH (10 mL) was mixed with a MeOH (10 mL) solution of KOH (3.3 mmol, 0.185 g). An aqueous (10 mL) solution of NiCl_2 (1.9 mmol, 0.247 g) was added dropwise under vigorous stirring to the resulting potassium salt. The mixture was stirred at room temperature for a further 3 h and left overnight. The resulting complex was extracted with CH_2Cl_2 , washed with water, and dried with anhydrous MgSO_4 . The solvent was removed under vacuum, and the product was purified by recrystallization from a 1:3 (v/v) mixture of CH_2Cl_2 and *n*-hexane. Yield: 1.072 g (87%). IR: $\tilde{\nu} = 956$ (POC), 1560 (SCN), 1235 (P=O), 3257 (NH) cm^{-1} . ^1H NMR (CDCl_3): $\delta = 7.32$ – 8.04 (m, 30 H, Ph), 9.15 (s, 2 H, PhNH) ppm. $^{31}\text{P}\{^1\text{H}\}$ NMR (CDCl_3): $\delta = -7.8$ ppm. ^1H NMR ($[\text{D}_6]\text{DMSO}$): $\delta = 5.07$ (br. s, 2 H, PhNH), 6.92– 7.71 (m, 30 H, Ph) ppm. $^{31}\text{P}\{^1\text{H}\}$ NMR ($[\text{D}_6]\text{DMSO}$): $\delta = -5.4$ ppm. UV/Vis (CH_2Cl_2): λ_{max} (ϵ , $\text{M}^{-1}\text{cm}^{-1}$) = 260 (26135), 321 (18120), 508 (218), 630 (185) nm. UV/Vis (DMSO): λ_{max} (ϵ , $\text{M}^{-1}\text{cm}^{-1}$) = 249 (25053), 303 (2425), 440 (65), 726 (12), 1124 (15) nm. $\text{C}_{38}\text{H}_{32}\text{N}_4\text{NiO}_6\text{P}_2\text{S}_2$ (825.45): calcd. C 55.29, H 3.91, N 7.11; found C 55.42, H 4.02, N 7.16.

$[\text{NiL}_2\text{pz}]_n$: An equimolar mixture of $[\text{NiL}_2]$ (0.5 mmol, 0.413 g) and pyrazine (0.5 mmol, 0.040 g) in benzene (10 mL) was stirred at room temperature for 10 min and left for slow evaporation of the solvent. Green rod-like crystals were formed during the next days. Yield (calculated for $[\text{NiL}_2\text{pz}]_n$): 0.326 g (72%). IR: $\tilde{\nu} = 968$ (POC), 1573 (SCN), 1135 (P=O), 3184 (NH) cm^{-1} . ^1H NMR (CDCl_3): $\delta = 4.18$ (s, 2 H, PhNH), 5.27– 6.11 (m, 30 H, Ph), 9.13– 9.84 (m, 4 H, pyrazine) ppm. $^{31}\text{P}\{^1\text{H}\}$ NMR (CDCl_3): $\delta = 24.2$ ppm. ^1H NMR ($[\text{D}_6]\text{DMSO}$): $\delta = 4.37$ (s, 2 H, PhNH), 5.47– 6.74 (m, 30 H, Ph), 9.42– 10.07 (m, 4 H, pyrazine) ppm. $^{31}\text{P}\{^1\text{H}\}$ NMR ($[\text{D}_6]\text{DMSO}$): $\delta = 26.1$ ppm. UV/Vis (CH_2Cl_2): λ_{max} (ϵ , $\text{M}^{-1}\text{cm}^{-1}$) = 252 (26775), 306 (2570), 452 (68), 722 (14), 1125 (17) nm. UV/Vis (DMSO): λ_{max} (ϵ , $\text{M}^{-1}\text{cm}^{-1}$) = 250 (26830), 310 (2545), 448 (64), 729 (13), 1119 (15) nm. $\text{C}_{42}\text{H}_{36}\text{N}_6\text{NiO}_6\text{P}_2\text{S}_2$ (905.54): calcd. C 55.71, H 4.01, N 9.28; found C 55.87, H 4.09, N 9.36.

Synthesis of TOP-Capped Nickel Nanoparticles: Complex $[\text{NiL}_2\text{pz}]_n$ (0.2 mmol, 0.181 g) was dissolved in tri-*n*-octylphosphine (TOP) (6 mL) and injected into hot hexadecylamine (HDA) (6.025 g, 25 mmol) at 190 °C. An initial decrease in temperature from 190 to about 175 °C was observed. The solution was then allowed to stabilize, and the reaction was continued for 45 min at 190 °C. After completion, the reaction mixture was cooled to 70 °C, and methanol was added to precipitate the nanoparticles. The solid was separated by centrifugation and washed five times with methanol. The resulting solid precipitates of TOP-capped nickel nanoparticles were dispersed in toluene for further analysis.

Crystal Structure Determination: X-ray data collections for HL and $[\text{NiL}_2\text{pz}]_n$ were performed with a Mar345 image plate detector by using Mo- K_α radiation (Zr-filter) at 150(2) K. The data were integrated with the crysAlisPro software.^[17] The implemented empirical absorption correction was applied. The structures were solved by direct methods with the SHELXS-97 program^[18] and refined by full-matrix least-squares on $|F^2|$ with SHELXL-97.^[18] Non-hydrogen atoms were anisotropically refined, and the hydrogen atoms were placed on calculated positions in riding mode with temperature factors fixed at 1.2 times the U_{eq} value of the parent atoms. Figures were generated with the program Mercury.^[19]

Crystal Data for HL: $\text{C}_{19}\text{H}_{17}\text{N}_2\text{O}_3\text{PS}$, $M_r = 384.38 \text{ g mol}^{-1}$, monoclinic, space group $P2_1/c$, $a = 16.2222(7) \text{ \AA}$, $b = 11.2641(4) \text{ \AA}$, $c = 10.2615(5) \text{ \AA}$, $\beta = 91.410(5)^\circ$, $V = 1874.50(14) \text{ \AA}^3$, $Z = 4$, $\rho = 1.623 \text{ g cm}^{-3}$, $\mu(\text{Mo-}K_\alpha) = 0.279 \text{ mm}^{-1}$, reflections: 14376 collected, 3436 unique, $R_{\text{int}} = 0.045$, $R_1(\text{all}) = 0.0579$, $wR_2(\text{all}) = 0.1544$.

Crystal Data for $[\text{NiL}_2\text{pz}]_n$: $\text{C}_{42}\text{H}_{36}\text{N}_6\text{NiO}_6\text{P}_2\text{S}_2$, $M_r = 905.54 \text{ g mol}^{-1}$, triclinic, space group $P\bar{1}$, $a = 13.238(7) \text{ \AA}$, $b = 13.993(4) \text{ \AA}$, $c = 15.354(9) \text{ \AA}$, $\alpha = 77.87(4)^\circ$, $\beta = 70.08(5)^\circ$, $\gamma = 74.89(4)^\circ$, $V = 2558(2) \text{ \AA}^3$, $Z = 2$, $\rho = 1.176 \text{ g cm}^{-3}$, $\mu(\text{Mo-}K_\alpha) = 0.568 \text{ mm}^{-1}$, reflections: 3741 collected, 1868 unique, $R_{\text{int}} = 0.149$, $R_1(\text{all}) = 0.1208$, $wR_2(\text{all}) = 0.3220$.

CCDC-983543 (for HL) and -983544 (for $[\text{NiL}_2\text{pz}]_n$) contain the supplementary crystallographic data for this paper. These data can be obtained free of charge from The Cambridge Crystallographic Data Centre via www.ccdc.cam.ac.uk/data_request/cif.

Supporting Information (see footnote on the first page of this article): Selected bond lengths and bond angles for HL, selected bond lengths and bond angles for $[\text{NiL}_2\text{pz}]_n$, selected hydrogen bond lengths and bond angles of HL, and $\pi\cdots\pi$ bond lengths (\AA) and angles ($^\circ$) for $[\text{NiL}_2\text{pz}]_n$.

Acknowledgments

We thank Wallonie-Bruxelles International (WBI, Belgium) for postdoctoral positions allocated to M. G. B. and D. A. S. This work was supported by COST (MP1202).

- [1] S. Kitagawa, S. Natarajan, *Eur. J. Inorg. Chem.* **2010**, 3685.
- [2] M. L. Foo, R. Matsuda, S. Kitagawa, *Chem. Mater.* **2014**, *26*, 310.
- [3] a) S. M. Cohen, Z. Q. Wang, *Chem. Soc. Rev.* **2009**, *38*, 1315; b) Z. B. Ma, B. Moulton, *Coord. Chem. Rev.* **2011**, *255*, 1623; c) E. Coronado, G. Mínguez Espallargas, *Chem. Soc. Rev.* **2013**, *42*, 1525; d) L. Fabbri, A. Poggi, *Chem. Soc. Rev.* **2013**, *42*, 1681; e) P. D. Frischmann, K. Mahata, F. Würthner, *Chem. Soc. Rev.* **2013**, *42*, 1847.
- [4] J. D. Rocca, W. Lin, *Eur. J. Inorg. Chem.* **2010**, 3725.
- [5] S. K. Henninger, F. Jeremias, H. Kummer, C. Janiak, *Eur. J. Inorg. Chem.* **2012**, 2625.
- [6] C. Kaes, A. Katz, M. W. Hosseini, *Chem. Rev.* **2000**, *100*, 3553.

- [7] W. Kaim, *Angew. Chem. Int. Ed. Engl.* **1983**, *22*, 171; *Angew. Chem.* **1983**, *95*, 201.
- [8] For examples: a) R. Rösler, C. Silvestru, G. Espinosa-Perez, I. Haiduc, R. Cea-Olivares, *Inorg. Chim. Acta* **1996**, *241*, 47; b) A. Silvestru, D. Bilec, R. Rosler, J. E. Drake, I. Haiduc, *Inorg. Chim. Acta* **2000**, *305*, 106; c) E. V. Garcia-Baez, M. J. Rozales-Hoz, H. Nöth, I. Haiduc, C. Silvestru, *Inorg. Chem. Commun.* **2000**, *3*, 173; d) S. D. Robertson, T. Chivers, J. Akhtar, M. Afzaal, P. O'Brien, *Dalton Trans.* **2008**, 7004; e) I. Haiduc, *J. Organomet. Chem.* **2001**, *623*, 29; f) A. Panneerselvam, M. A. Malik, M. Afzaal, P. O'Brien, M. Helliwell, *J. Am. Chem. Soc.* **2008**, *130*, 2420; g) N. Levesanos, S. D. Robertson, D. Maganas, C. P. Raptopoulou, A. Terzis, P. Kyritsis, T. Chivers, *Inorg. Chem.* **2008**, *47*, 2949; h) D. Maganas, A. Grigoropoulos, S. S. Staniland, S. D. Chatziefthimiou, A. Harrison, N. Robertson, P. Kyritsis, F. Neese, *Inorg. Chem.* **2010**, *49*, 5079; i) E. Ferentinos, D. Maganas, C. P. Raptopoulou, A. Terzis, V. Psycharis, N. Robertson, P. Kyritsis, *Dalton Trans.* **2011**, *40*, 169.
- [9] For examples: a) K. R. Koch, O. Hallale, S. A. Bourne, J. Miller, J. Bacsa, *J. Mol. Struct.* **2001**, *561*, 185; b) S. A. Bourne, O. Hallale, K. R. Koch, *Cryst. Growth Des.* **2005**, *5*, 307; c) O. Hallale, S. A. Bourne, K. R. Koch, *New J. Chem.* **2005**, *29*, 1416; d) O. Hallale, S. A. Bourne, K. R. Koch, *CrystEngComm* **2005**, *7*, 161.
- [10] a) F. D. Sokolov, S. V. Baranov, D. A. Safin, F. E. Hahn, M. Kubiak, T. Pape, M. G. Babashkina, N. G. Zabirow, J. Galezowska, H. Kozlowski, R. A. Cherkasov, *New J. Chem.* **2007**, *31*, 1661; b) F. D. Sokolov, V. V. Brusko, D. A. Safin, R. A. Cherkasov, N. G. Zabirow, "Coordination Diversity of *N*-Phosphorylated Amides and Ureas towards VIII B Group Cations" in *Transition Metal Chemistry: New Research* (Eds.: B. Varga, L. Kis), **2008**, Nova Science Publishers Inc., Hauppauge NY, USA, p. 101; c) D. A. Safin, F. D. Sokolov, L. Szyrwiel, M. G. Babashkina, T. R. Gimadiev, F. E. Hahn, H. Kozlowski, D. B. Krivolapov, I. A. Litvinov, *Polyhedron* **2008**, *27*, 2271; d) D. A. Safin, F. D. Sokolov, T. R. Gimadiev, V. V. Brusko, M. G. Babashkina, D. R. Chubukaeva, D. B. Krivolapov, I. A. Litvinov, *Z. Anorg. Allg. Chem.* **2008**, *634*, 967; e) D. A. Safin, M. G. Babashkina, A. Klein, F. D. Sokolov, S. V. Baranov, T. Pape, F. E. Hahn, D. B. Krivolapov, *New J. Chem.* **2009**, *33*, 2443; f) M. G. Babashkina, D. A. Safin, M. Bolte, A. Klein, *Inorg. Chem. Commun.* **2009**, *12*, 678; g) D. A. Safin, M. Bolte, M. G. Babashkina, H. Kozlowski, *Polyhedron* **2010**, *29*, 488; h) D. A. Safin, M. G. Babashkina, M. Bolte, A. Klein, *Inorg. Chim. Acta* **2011**, *365*, 32; i) M. G. Babashkina, D. A. Safin, M. Bolte, M. Srebro, M. Mitoraj, A. Uthe, A. Klein, M. Kockerling, *Dalton Trans.* **2011**, *40*, 3142; j) D. A. Safin, M. G. Babashkina, M. Bolte, F. E. Hahn, *Dalton Trans.* **2011**, *40*, 4806; k) M. G. Babashkina, D. A. Safin, M. Srebro, P. Kubisiak, M. P. Mitoraj, M. Bolte, Y. Garcia, *CrystEngComm* **2011**, *13*, 5321; l) M. G. Babashkina, D. A. Safin, K. Robeyns, Y. Garcia, *Dalton Trans.* **2012**, *41*, 1451; m) M. G. Babashkina, D. A. Safin, Y. Garcia, *Dalton Trans.* **2012**, *41*, 2234; n) M. G. Babashkina, D. A. Safin, M. Srebro, P. Kubisiak, M. P. Mitoraj, M. Bolte, Y. Garcia, *CrystEngComm* **2012**, *14*, 370; o) M. G. Babashkina, D. A. Safin, M. Srebro, P. Kubisiak, M. P. Mitoraj, M. Bolte, Y. Garcia, *Eur. J. Inorg. Chem.* **2013**, 545; p) D. A. Safin, M. G. Babashkina, P. Kubisiak, M. P. Mitoraj, K. Robeyns, E. Goovaerts, Y. Garcia, *Dalton Trans.* **2013**, *42*, 5252; q) D. A. Safin, M. G. Babashkina, K. Robeyns, M. P. Mitoraj, P. Kubisiak, M. Brela, Y. Garcia, *CrystEngComm* **2013**, *15*, 7845; r) D. A. Safin, M. G. Babashkina, K. Robeyns, M. Rouzières, R. Clérac, Y. Garcia, *Dalton Trans.* **2013**, *42*, 16470.
- [11] J. Coates, "Interpretation of Infrared Spectra, A Practical Approach" in *Encyclopedia of Analytical Chemistry* (Ed.: R. A. Meyers), **2000**, John Wiley & Sons Ltd, Chichester, pp. 10815–10837.
- [12] a) R. H. Dingle, *Inorg. Chem.* **1971**, *10*, 1141; b) S. F. A. Kettle, *Physical Inorganic Chemistry: A Coordination Chemistry Approach*, Springer Spektrum, Berlin, Heidelberg, **1996**, p. 175.

- [13] For example: a) R. C. Luckay, X. Sheng, C. E. Strasser, H. G. Raubenheimer, D. A. Safin, M. G. Babashkina, A. Klein, *Dalton Trans.* **2009**, 4646; b) R. C. Luckay, X. Sheng, C. E. Strasser, H. G. Raubenheimer, D. A. Safin, M. G. Babashkina, A. Klein, *Dalton Trans.* **2009**, 8227; c) M. G. Babashkina, D. A. Safin, M. Bolte, Y. Garcia, *Dalton Trans.* **2012**, 41, 3223; d) M. G. Babashkina, D. A. Safin, K. Robeyns, A. Brzuszkiewicz, H. Kozlowski, Y. Garcia, *CrystEngComm* **2012**, 14, 1324.
- [14] a) E. O. Wollan, J. W. Cable, W. C. Koehler, *J. Phys. Chem. Solids* **1963**, 24, 1141; b) S. S. M. Tavares, S. Miraglia, A. Lafuente, D. Fruchart, *J. Magn. Magn. Mater.* **2002**, 242–245, 898.
- [15] R. P. Furstenuau, G. McDougall, M. A. Langell, *Surf. Sci.* **1985**, 150, 55.
- [16] Y. Kang, M. Li, Y. Cai, M. Cargnello, R. E. Diaz, T. R. Gordon, N. L. Wieder, R. R. Adzic, R. J. Gorte, E. A. Stach, C. B. Murray, *J. Am. Chem. Soc.* **2013**, 135, 2741.
- [17] *Oxford Diffraction Data Collection and Data Reduction*, Version 171.34.40, **2011**.
- [18] G. M. Sheldrick, *Acta Crystallogr., Sect. A* **2008**, 64, 112.
- [19] I. J. Bruno, J. C. Cole, P. R. Edgington, M. Kessler, C. F. Macrae, P. McCabe, J. Pearson, R. Taylor, *Acta Crystallogr., Sect. B* **2002**, 58, 389.

Received: April 6, 2014
Published Online: June 3, 2014